THE UNIVERSITY of EDINBURGH

Edinburgh Research Explorer

Why is the antipodal effect in closo-1-SB9H9 so large? A possible explanation based on the geometry from the concerted use of gas electron diffraction and computational methods

OPEN ACCESS

Why is the antipodal effect in *closo*-1-SB₉H₉ so large? A possible explanation based on the geometry from the concerted use of gas electron diffraction and computational methods†

Drahomír Hnyk,[*a] **Derek A. Wann,**[b] **Josef Holub,**[a] **Svein Samdal**[c] **and David W. H. Rankin**[b]

The molecular structure of 1-thia-*closo*-decaborane(9), 1-SB₉H₉, has been determined by the concerted use of gas electron diffraction and quantum-chemical calculations. Assuming C_{4v} symmetry, the cage structure was distorted from a symmetrically bicapped square antiprism (D_{4d} symmetry) mainly through substantial expansion of the tetragonal belt of boron atoms adjacent to sulfur. The S–B and (B–B)$_{mean}$ distances are well determined with r_{h1} = 193.86(14) and 182.14(8) pm, respectively. Geometrical parameters calculated using the MP2(full)/6-311++G** method and at levels reported earlier [MP2(full)/6-311G**, B3LYP/6-311G** and B3LYP/cc-pVQZ], as well as calculated vibrational amplitudes and ¹¹B NMR chemical shifts, are in good agreement with the experimental findings. In particular, the so-called antipodal chemical shift of apical B(10) (71.8 ppm) is reproduced well by the GIAO-MP2 calculations and its large magnitude is schematically accounted for, as is the analogous antipodal chemical shift of B(12) in the twelve-vertex *closo*-1-SB₁₁H₁₁.

Introduction

In the same way that an icosahedron represents the fundamental building block for twelve-vertex *closo* systems, the so-called Archimedes bicapped antiprism is known to be the building block for ten-vertex *closo* species. By replacing (BH)²⁻ vertices in the archetypal ten-vertex *closo* species, B₁₀H₁₀²⁻, with various isoelectronic moieties, a number of ten-vertex *closo* heteroboranes are formed in accordance with Wade's rules.[1] For instance, S is isoelectronic with (BH)²⁻ and its incorporation into this antiprismatic structure yields 1-thia-*closo*-decaborane(9), 1-SB₉H₉ (**1**), a molecule that was first synthesized many years ago.[1] This C_{4v}-symmetrical thiaborane has also been the subject of several structural studies. Its PES spectrum was recorded and interpreted using semiempirical quantum-chemical methods.[2,3] Molecular geometries calculated using Hartree–Fock theory have subsequently been reported,[4] as well as calculations carried out at higher levels of theory (MP2, B3LYP).[5] These last calculations were performed in conjunction with microwave spectroscopy to determine the molecular structure of the thiaborane in the gas phase. Gas electron diffraction (GED) is similarly able to derive

structures in the vapour phase and the availability of rotational constants[5] for various isotopomers of 1-SB₉H₉ might allow these data to be introduced as restraints into the GED refinement, with the aim of enabling the determination of a particularly accurate experimental geometry. Here we determine this experimental geometry in the gas phase and compare it with that established for the dimeric derivative of the thiaborane, 2,2′-(1-SB₉H₈)₂, in the solid state by X-ray diffraction.[2]

Because the molecule possesses C_{4v} symmetry there are three signals in the ¹¹B NMR spectrum of **1**. The most striking feature of these resonances is the ¹¹B NMR chemical shift of atom B(10) at 71.8 ppm.[5] To the best of our knowledge, this is the highest frequency ¹¹B chemical shift, this atom being antipodally coupled with sulfur.[2] The apical boron atom in the icosahedral analogue of **1**, 1-SB₁₁H₁₁, which is also antipodally coupled with sulfur, resonates at *ca.* 19 ppm.[2] As well as determining the molecular structure of **1** using a combination of GED and quantum-chemical calculations, we have outlined a possible explanation of the difference between the δ(¹¹B) values associated with the antipodally coupled boron and sulfur atoms in **1** and in 1-SB₁₁H₁₁.

Results and discussion

GED study

On the basis of the calculations described above, C_{4v} symmetry was assumed when writing the model describing 1-SB₉H₉. The geometry was described in terms of ten refinable parameters, comprising eight bond lengths and differences and two angles

aInstitute of Inorganic Chemistry of the ASCR, v.v.i., No. 1001, CZ-250 68, Husinec-Řež, Czech Republic. E-mail: hnyk@iic.cas.cz
bSchool of Chemistry, University of Edinburgh, West Mains Road, Edinburgh, UK EH9 3JJ
cCenter for Theoretical and Computational Chemistry (CTCC), Department of Chemistry, University of Oslo, P. O. Box 1033, Blindern, NO-0315, Oslo, Norway
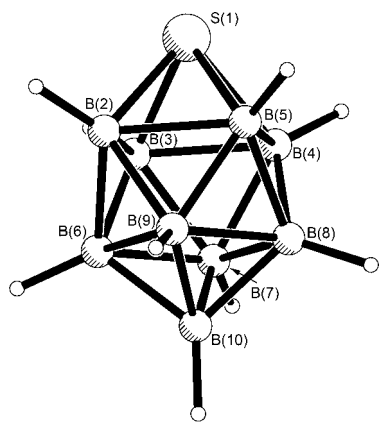
Table 1

Table 1 Refined (r_{h1}) and calculated (r_e) geometric parameters for 1-SB_9H_9 from the combined GED and *ab initio* refinement[a,b]

	Parameter	r_{h1}	r_e	Restraint
Independent				
p_1	rS–B	193.86(14)	193.5	—
p_2	rB–B average	182.14(8)	181.0	—
p_3	rB–B difference 1	15.5(2)	14.0	14.0(5)
p_4	rB–B difference 2	8.9(3)	9.2	9.2(5)
p_5	rB–B difference 3	−6.4(4)	−6.3	−6.3(5)
p_6	rB–H mean	121.3(3)	118.4	—
p_7	rB–H difference 1	−0.5(5)	−0.4	−0.4(5)
p_8	rB–H difference 2	−0.2(5)	−0.3	−0.3(5)
p_9	∠SB(2)H	110.7(9)	110.6	110.6(10)
p_{10}	∠B(10)B(8)H	119.3(8)	120.3	120.3(10)
Dependent				
p_{11}	B(2)–B(3)	194.50(15)	192.2	—
p_{12}	B(2)–B(6)	179.0(2)	178.0	—
p_{13}	B(6)–B(7)	185.7(3)	185.1	—
p_{14}	B(6)–B(10)	172.6(3)	171.7	—

[a] Refers to an MP2(full)/6-311++G** calculation. [b] Distances (r) are in pm, and angles (∠) are in degrees. See text for parameter definitions and Fig. 1 for atom numbering. The figures in parentheses are the estimated standard deviations of the last digits.

(Table 1). The atom numbering used in the descriptions of the parameters is shown in Fig. 1. The S–B bond lengths were identical and described using p_1. Four different B–B bonds were identified in the structure [B(2)–B(3), B(2)–B(6), B(6)–B(7) and B(6)–B(10)] and these were described using the weighted average of the distances [to account for the fact that symmetry equivalents of B(2)–B(6) occur twice as often as the others] and differences between them. The formal definitions of p_2 to p_5 were as follows

$$p_2 = \{[B(2)–B(3)] + 2\times[B(2)–B(6)] + [B(6)–B(7)] + [B(6)–B(10)]\}/5$$

$$p_3 = [B(2)–B(3)] − \{2\times[B(2)–B(6)] + [B(6)–B(7)] + [B(6)–B(10)]\}/4$$

$$p_4 = [B(6)–B(7)] − \{2\times[B(2)–B(6)] + [B(6)–B(10)]\}/3$$

$$p_5 = [B(6)–B(10)] − [B(2)–B(6)]$$

The four different B–B bond lengths were then described using p_2 to p_5 as follows:

B(2)–B(3) = $p_2 + 4\times p_3/5$

B(2)–B(6) = $p_2 − p_3/5 − p_4/4 − p_5/3$

Fig. 1 The molecular structure, including numbering scheme, for 1-SB_9H_9. Hydrogen atoms are given the same number as the boron to which they are attached [*e.g.* H(2) is bonded to B(2)].

B(6)–B(7) = $p_2 − p_3/5 + 3\times p_4/4$

B(6)–B(10) = $p_2 − p_3/5 − p_4/4 + 2\times p_5/3$

An average B–H bond length and two differences (p_{6-8}) were defined as follows:

$$p_6 = \{[B(10)–H] + 4\times[B(6)–H] + 4\times[B(2)–H]\}/9$$

$$p_7 = [B(10)–H] − \{[B(6)–H] + [B(2)–H]\}/2$$

$$p_8 = [B(6)–H] − [B(2)–H]$$

The angles defining the positions of the different hydrogen atoms were described by S–B(2)–H (p_9) and B(10)–B(8)–H (p_{10}).

All ten independent geometric parameters were refined by least squares with restraints applied to several parameters (Table 1). Additionally, six amplitudes of vibration (or groups of amplitudes tied to one refining amplitude) were refined. See Table S2† for a list of amplitudes of vibration. No amplitude restraints were required. The success of the refinement can be assessed numerically using the final R factor, which was $R_G = 0.048$ ($R_D = 0.038$), and visually using the goodness of fit of the radial-distribution and difference curves as seen in Fig. 2, and the molecular-scattering intensity curves (Fig. S1†). The least-squares correlation matrix is given in Table S3† and coordinates for the final GED structure and for the calculated MP2(full)/6-311++G** structure are given in Tables S4 and S5,† respectively.
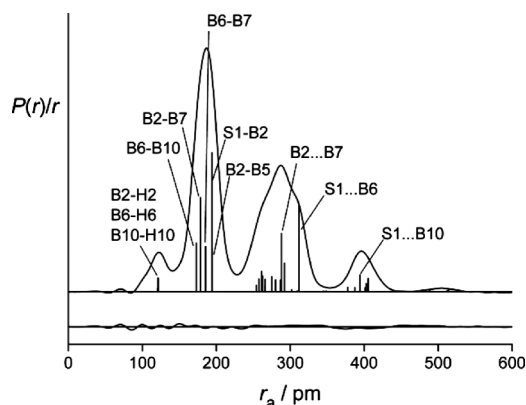
Fig. 2 Experimental radial-distribution curve and theoretical-minus-experimental difference curve for the refinement of 1-SB_9H_9. Before Fourier inversion the data were multiplied by $s\cdot exp(−0.00002s^2)/(Z_S − f_S)(Z_B − f_B)$.

Rotational constants are available for several different isotopomers of 1-SB_9H_9, with both sulfur and boron having been isotopically substituted.[5] For each of the symmetric tops $^{32}S^{11}B_9H_9$ (**1**), $^{33}S^{11}B_9H_9$ (**2**), $^{34}S^{11}B_9H_9$ (**3**) and $^{32}S^{10}B(10)^{11}B_8H_9$ (**4**), one rotation constant has been determined. Attempts were made to use these rotation constants as extra data in the refinements. However, it proved impossible to use the rotation constants without severely distorting the structure. This was gauged by the GIAO/MP2 calculations performed for that experimental geometry, which give for B(10) an ^{11}B chemical shift of 80.4 ppm. Such a discrepancy between the theoretical and experimental ^{11}B NMR chemical shifts might lead one to doubt the experimental geometry.[6] In addition to that, the value is itself very close to a much less reliable GIAO/HF value (82.5 ppm) calculated for the final geometry we report. The GIAO/MP2 calculations showed that the chemical shift of the B(10) atom is very heavily reliant on the positions of the hydrogen atoms, which were not determined in the original microwave spectroscopy experiment. As a consequence, the final refinement

was therefore performed using only GED data, supplemented with *ab initio* SARACEN restraints.[7]

There is a substantial expansion of the square of boron atoms adjoining sulfur, with $r[B(2)–B(3)] = 194.60(23)$ pm. (In the original MW study this parameter was determined to be 193.7(1) pm[5] and in the dimeric derivative 2,2′-(1-SB_9H_8)$_2$ it is 193 pm.[2]) This expansion is more pronounced than that of the pentagonal belt of boron atoms in 1-$SB_{11}H_{11}$,[4] where the B–B distance determined using GED was 190.5(4) pm. The opposite trend applies to the S–B distance: 193.13(14) pm (MW: 194.4(2); the dimer: 192 pm) *vs.* 201.0(5) pm in 1-$SB_{11}H_{11}$.[4] There are slight discrepancies between GED and MW values of the B(2)–B(6) and B(6)–B(10) nearest-neighbour separations, the MW values being 176.5(3) and 170.7(1) pm, respectively. It should be noted the B(2)–B(6) and equivalent bonds connect boron atoms that are bonded to a total of eight hydrogen atoms. As these hydrogen-atom positions were not determined using the MW data this adds weight to our decision not to use the rotation constants as extra data. This speculation applies to a lesser extent to the B(6)–B(10)-type bonds [five hydrogen atoms are bonded to B(6) and its equivalent atoms and to B(10)].

Previous gas-phase studies of boron clusters with *closo* structures have determined that amplitudes of vibration both for adjacent atom pairs and for those more widely separated have remarkably similar values. For example, vibrational amplitudes associated with S–B and with the icosahedral body diagonal S···B in 1-$SB_{11}H_{11}$ were determined to be 7.1(4) and 5.8(3) pm.[4] This similarity is also found for **1**, for which u(S–B) and u[S···B(10)] refined to 7.1(3) and 6.5(3) pm, respectively. This shows that *closo* systems are quite rigid and the fact that the lowest calculated vibrational frequencies for **1** are higher than 300 cm^{-1} confirms this rigidity.

The final experimental geometry of **1** was computed to be 10.4 kJ mol^{-1} higher in energy than that of the theoretical structure [MP2(full)/6-311++G**]. However, a major part of this excess energy may be ascribed to the hydrogen placements; the difference in relative energy was reduced to 1.5 kJ mol^{-1} when the structure of the SB_9 skeleton was fixed at its experimental geometry and the hydrogen positions were optimized at the MP2(full)/6-311++G** level. Both the similarity in energy and the NMR fit (as revealed in Table 2) indicate that the SARACEN electron-diffraction refinement affords a very good representation of the molecular structure of free 1-SB_9H_9.

The chemical shifts calculated using coordinates that were themselves calculated at the MP2(full)/6-311++G** are considered to be the best that we have calculated and they agree extremely well with chemical shifts calculated from the final GED geometry. Two sets of experimental chemical shifts are also available for comparison.[5,8] The values from these two NMR experiments are quite different and the reason for this difference might be based on entirely different solvents used: benzene is an aromatic solvent with magnetic anisotropy and a quadrupole moment, whereas $CDCl_3$ is a polar solvent with a dipole moment. Upon moving from the aliphatic to the aromatic solvent, not negligible changes in NMR patters were observed for some borane cages.[9]

The ^{11}B NMR chemical shift for B(10) of 74.5 ppm[8] (shown in Table 2) and the corresponding calculated value [76.2 ppm calculated with GIAO-MP2/II using MP2(full)/6-311++G** coordinates] is the highest frequency chemical shift observed for

Table 2 Calculated and experimental ^{11}B NMR chemical shifts for 1-SB_9H_9

$\delta(^{11}B)$/ppm

	B(2–5)	B(6–9)	B(10)
GIAO-MP2/II[a]	−4.2	−19.3	78.5
GIAO-MP2/II[b]	−3.7	−19.7	78.7
GIAO-MP2/II[c]	−5.2	−20.0	76.2
GIAO-MP2/II[d]	−4.5	−19.6	76.9
Exp. (in $CDCl_3$)[5]	−7.6	−20.9	71.8
Exp. (in C_6D_6)[8]	−4.8	−17.6	74.5

[a] B3LYP/cc-pVTZ. [b] B3LYP/6-311++G**. [c] MP2(full)/6-311+G**. [d] GED.

this class of materials. To explain why the antipodal effect in the ten-vertex species is larger than in the twelve-vertex one (*i.e.* in 1-$SB_{11}H_{11}$)[4] we might speculate that the mechanism is the same in both cases: the occurrence of paramagnetic contributions to the magnetic shielding constants. These contributions arise from the coupling of suitable occupied and unoccupied molecular orbitals with large coefficients on the antipodal atom. The heteroatom leads to a better overlap due to polarization of the occupied MO (HOMO for 1-SB_9H_9 and HOMO-2 for 1-$SB_{11}H_{11}$, Fig. 3) towards the antipodal atom. The energetic separation between these coupled pairs of occupied and virtual MOs is larger in 1-$SB_{11}H_{11}$ (13.8 eV at 6-31G*) than in 1-SB_9H_9 (12.3 eV at the same level), which is consistent with much larger deshielding for the latter.

1a   **1b**

2a   **2b**
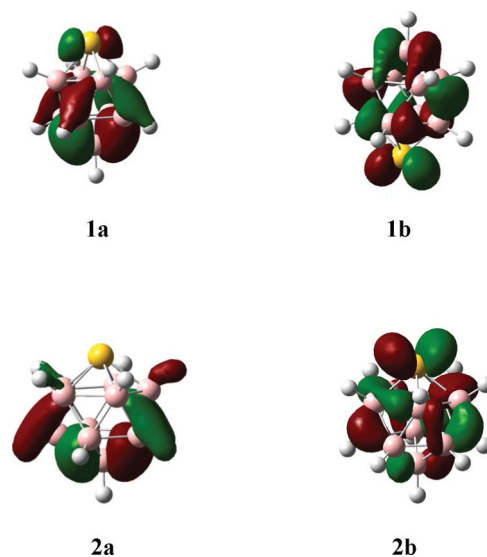
Fig. 3 Key molecular orbitals for paramagnetic contributions to the shielding tensor of the antipodal boron atom: HOMO and LUMO for 1-SB_9H_9 (**1a** and **1b**, respectively) and HOMO-1 and LUMO for 1-$SB_{11}H_{11}$ (**2a** and **2b**, respectively). Only one of each degenerate pair is shown.

The calculated nucleus-independent chemical shift (NICS)[10] for 1-SB_9H_9 is −22.9 ppm (GIAO-MP2/II). Such a value could mean that this species belongs to the group of the so-called three-dimensional aromatic systems,[11] as was the case with, for example, *closo*-2,1- and 6,1-PCB_8H_9.[12] Molecular structure determinations of other three-dimensional aromatics are in progress.

Experimental

Synthesis and NMR measurements

In a typical experiment, freshly sublimed *nido*-thiaborane 6-SB_9H_{11} (2.80 g, 20 mmol) was placed under an argon atmosphere into a stainless autoclave and heated at 400 °C overnight. After cooling down, the autoclave was connected to a dry-ice finger sublimator and the reaction mixture was sublimed at 50 °C. Column chromatography on silica using hexane as the eluent led to the isolation of one main colourless product, identified as the *closo*-thiaborane 1-SB_9H_9. The yield was 1.87 g (68%). ^{11}B NMR measurements are described in a great detail in ref. 5

Gas electron diffraction (GED)

Electron-diffraction data were recorded using the Balzers Eldigraph KD-G2 instrument at the University of Oslo[13,14] on Kodak electron image plates with nozzle-tip temperatures of between 65 and 68 °C for the middle camera data and between 68 and 73 °C for the long camera data. The accelerating voltage of the electron beam was 42 kV and the voltage/distance calibration was performed using benzene as a reference. The weighting points for the off-diagonal weight matrices, correlation parameters and scale factors for both camera distances are given in Table S1.† The least-squares refinement process was carried out using the ed@ed v3.0 program[15] employing the scattering factors of Ross *et al.*[16]

Computational methods

Along with the microwave study[5] of 1-SB_9H_9 a series of high-level calculations were reported. These calculations at the MP2(full)/6-311G**, B3LYP/6-311G** and B3LYP/cc-pVQZ levels found the structure to have C_{4v} symmetry. Using the resources of the UK National Service for Computational Chemistry Software (NSCCS)[17] running the Gaussian 03 suite of programs,[18] we extended these calculations to the MP2(full)/6-311++G** and B3LYP/6-311++G** levels.

Force constants were calculated at the B3LYP/aug-cc-pVTZ level and subsequently used, along with the program SHRINK,[19] to obtain initial amplitudes of vibration and curvilinear distance correction terms for use in the GED refinement.

NMR chemical shifts were calculated using the GIAO-MP2 method,[20] which is incorporated in the Gaussian 03 program. The individual gauge for localized orbitals (IGLO-II) basis sets were used for all atoms.[21]

Acknowledgements

Notes and references

1 K. Wade, *Adv. Inorg. Chem. Radiochem.*, 1976, **18**, 1.
2 W. R. Pretzer, T. K. Hilty and R. W. Rudolph, *Inorg. Chem.*, 1975, **14**, 2459.
3 For the meaning of the antipodal effect in *closo*-heteroboranes see: M. Bühl, P. v. R. Schleyer, Z. Havlas, D. Hnyk and S. Heřmánek, *Inorg. Chem.*, 1991, **30**, 3107, and references therein.
4 D. Hnyk, E. Vajda, M. Bühl and P. v. R. Schleyer, *Inorg. Chem.*, 1992, **31**, 2464.
5 H. Møllendal, S. Samdal, J. Holub and D. Hnyk, *Inorg. Chem.*, 2002, **41**, 4574. Difficulties in determining the structures from microwave spectroscopy due to a large number of $^{10}B/^{11}B$ isotopomers are also mentioned in; D. Hnyk and D. W. H. Rankin, *Dalton Trans.*, 2009, 585.
6 See, for example, M. Bühl and P. v. R. Schleyer, *J. Am. Chem. Soc.*, 1992, **114**, 477.
7 A. J. Blake, P. T. Brain, H. McNab, J. Miller, C. A. Morrison, S. Parsons, D. W. H. Rankin, H. E. Robertson and B. A. Smart, *J. Phys. Chem.*, 1996, **100**, 12280; P. T. Brain, C. A. Morrison, S. Parsons and D. W. H. Rankin, *J. Chem. Soc., Dalton Trans.*, 1996, 4589; N. W. Mitzel and D. W. H. Rankin, *Dalton Trans.*, 2003, 3650.
8 W. L. Smith, B. J. Meneghelli, D. A. Thompson, P. Klymko, N. McClure, M. Bower and R. W. Rudolph, *Inorg. Chem.*, 1977, **16**, 3008; W. R. Pretzer and R. W. Rudolph, *J. Am. Chem. Soc.*, 1976, **98**, 1441.
9 E. J. M. Hamilton, R. G. Kulthsyev, B. Du, E. A. Meyers, S. Liu, Ch. M. Hadad and S. G. Shore, *Chem.–Eur. J.*, 2006, **12**, 2571 and references therein.
10 NICS is a three-dimensional aromaticity probe based on negative absolute magnetic shieldings at ring or cage centres: P. v. R. Schleyer, C. Maercker, A. Dransfeld, H. Jiao and N. J. R. Hommes, *J. Am. Chem. Soc.*, 1996, **118**, 6317.
11 For the three-dimensional aromaticity of boron clusters see, for example, P. v. R. Schleyer and K. Najafian, *Inorg. Chem.*, 1998, **37**, 3454.
12 J. Holub, M. Bakardjiev, B. Štíbr, D. Hnyk, O. L. Tok and B. Wrackmeyer, *Inorg. Chem.*, 2002, **41**, 2817.
13 W. Zeil, J. Haase and L. Wegmann, *Z. Instrumentenkd.*, 1966, **74**, 84.
14 O. Bastiansen, R. Graber and L. Wegmann, *Balzers High Vak. Rep.*, 1969, **25**, 1.
15 S. L. Hinchley, H. E. Robertson, K. B. Borisenko, A. R. Turner, B. F. Johnston, D. W. H. Rankin, M. Ahmadian, J. N. Jones and A. H. Cowley, *Dalton Trans.*, 2004, 2469.
16 A. W. Ross, M. Fink and R. Hilderbrandt, *International Tables for Crystallography*, (Ed.) A. J. C. Wilson, Kluwer Academic Publishers, Dordrecht, Netherlands, 1992, vol. C, p. 245.
17 National Service for Computational Chemistry Software (NSCCS). URL http://www.nsccs.ac.uk.
18 M. J. Frisch, G. W. Trucks, H. B. Schlegel, G. E. Scuseria, M. A. Robb, J. R. Cheeseman, J. A. Montgomery, Jr., T. Vreven, K. N. Kudin, J. C. Burant , J. M. Millam, S. S. Iyengar, J. Tomasi, V. Barone, B. Mennucci, M. Cossi, G. Scalmani, N. Rega, G. A. Petersson, H. Nakatsuji, M. Hada, M. Ehara, K. Toyota, R. Fukuda, J. Hasegawa, M. Ishida, T. Nakajima, Y. Honda, O. Kitao, H. Nakai, M. Klene, X. Li, J. E. Knox, H. P. Hratchian, J. B. Cross, C. Adamo, J. Jaramillo, R. Gomperts, R. E. Stratmann, O. Yazyev, A. J. Austin, R. Cammi, C. Pomelli, J. W. Ochterski, P. Y. Ayala, K. Morokuma, G. A. Voth, P. Salvador, J. J. Dannenberg, V. G. Zakrzewski, S. Dapprich, A. D. Daniels, M. C. Strain, O. Farkas, D. K. Malick, A. D. Rabuck, K. Raghavachari, J. B. Foresman, J. V. Ortiz, Q. Cui, A. G. Baboul, S. Clifford, J. Cioslowski, B. B. Stefanov, G. Liu, A. Liashenko, P. Piskorz, I. Komaromi, R. L. Martin, D. J. Fox, T. Keith, M. A. Al-Laham, C. Y. Peng, A. Nanayakkara, M. Challacombe, P. M. W. Gill, B. Johnson, W. Chen, M. W. Wong, C. Gonzalez and J. A. Pople, *Gaussian 03, Revision C.02*, Gaussian Inc., Pittsburgh PA, 2004.
19 A. Sipachev, *THEOCHEM*, 1985, **121**, 143; V. A. Sipachev, *J. Mol. Struct.*, 2001, **567**, 67.
20 R. Ditchfield, *Mol. Phys.*, 1974, **27**, 789; K. Wolinski, J. F. Hilton and P. Pulay, *J. Am. Chem. Soc.*, 1990, **112**, 8251; J. Gauss, *J. Chem. Phys.*, 1993, **99**, 3629.
21 W. Kutzelnigg, U. Fleischer and M. Schindler, *NMR Basic Principles and Progress*, Springer, Berlin, 1990, vol. 23, pp. 165-262.